

Hydrogeomorphology Influences Soil Nitrogen and Phosphorus Mineralization in Floodplain Wetlands

Gregory B. Noe, Cliff R. Hupp & Nancy B. Rybicki

Ecosystems

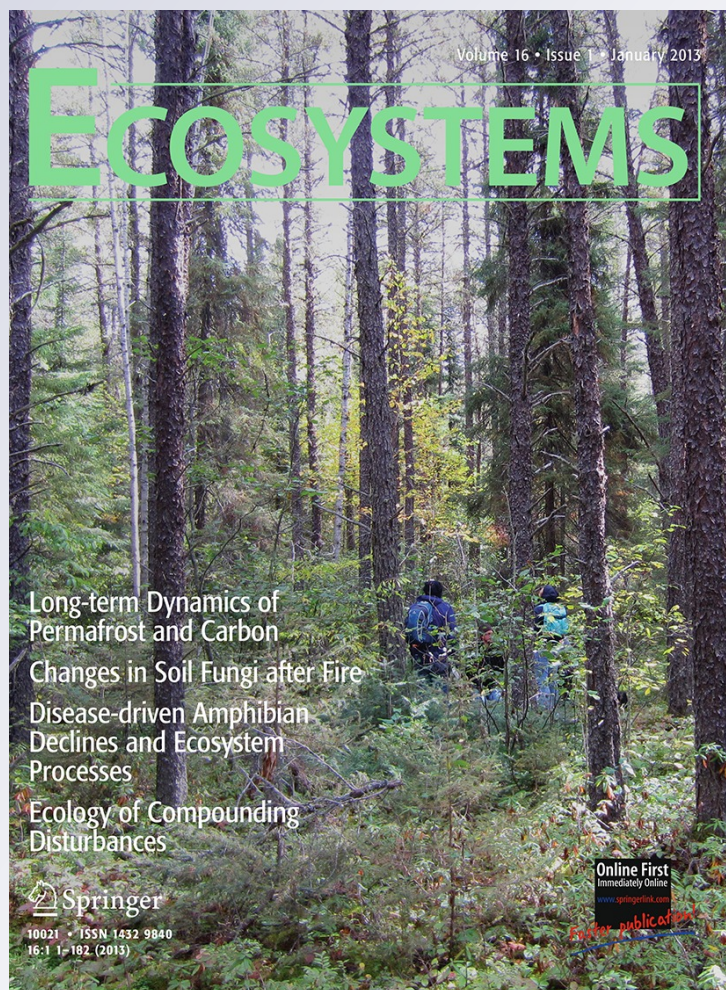
ISSN 1432-9840

Volume 16

Number 1

Ecosystems (2013) 16:75-94

DOI 10.1007/s10021-012-9597-0



Your article is protected by copyright and all rights are held exclusively by Springer Science+Business Media, LLC (outside the USA). This e-offprint is for personal use only and shall not be self-archived in electronic repositories. If you wish to self-archive your work, please use the accepted author's version for posting to your own website or your institution's repository. You may further deposit the accepted author's version on a funder's repository at a funder's request, provided it is not made publicly available until 12 months after publication.

Hydrogeomorphology Influences Soil Nitrogen and Phosphorus Mineralization in Floodplain Wetlands

Gregory B. Noe,* Cliff R. Hupp, and Nancy B. Rybicki

U.S. Geological Survey, 430 National Center, Reston, Virginia 20192, USA

ABSTRACT

Conceptual models of river–floodplain systems and biogeochemical theory predict that floodplain soil nitrogen (N) and phosphorus (P) mineralization should increase with hydrologic connectivity to the river and thus increase with distance downstream (longitudinal dimension) and in lower geomorphic units within the floodplain (lateral dimension). We measured rates of in situ soil net ammonification, nitrification, N, and P mineralization using monthly incubations of modified resin cores for a year in the forested floodplain wetlands of Difficult Run, a fifth order urban Piedmont river in Virginia, USA. Mineralization rates were then related to potentially controlling ecosystem attributes associated with hydrologic connectivity, soil characteristics, and vegetative inputs. Ammonification and P mineralization were greatest in the wet backswamps, nitrification was greatest in the dry levees, and net N mineralization was greatest in the intermediately wet toe-slopes. Nitrification also was greater in the headwater sites than downstream sites, whereas

ammonification was greater in downstream sites. Annual net N mineralization increased with spatial gradients of greater ammonium loading to the soil surface associated with flooding, soil organic and nutrient content, and herbaceous nutrient inputs. Annual net P mineralization was associated negatively with soil pH and coarser soil texture, and positively with ammonium and phosphate loading to the soil surface associated with flooding. Within an intensively sampled low elevation flowpath at one site, sediment deposition during individual incubations stimulated mineralization of N and P. However, the amount of N and P mineralized in soil was substantially less than the amount deposited with sedimentation. In summary, greater inputs of nutrients and water and storage of soil nutrients along gradients of river–floodplain hydrologic connectivity increased floodplain soil nutrient mineralization rates.

Key words: nutrient; geomorphology; hydrologic connectivity; river; riparian; biogeochemistry.

Received 29 June 2012; accepted 19 August 2012;
published online 25 September 2012

Electronic supplementary material: The online version of this article (doi:10.1007/s10021-012-9597-0) contains supplementary material, which is available to authorized users.

Author Contributions: GBN analyzed the data and wrote the manuscript. GBN led the study and was responsible for the collection of all soil data, CRH was responsible for the collection of all hydrologic and geomorphic data, and NBR was responsible for the collection of all vegetation data. All authors conceived the original study design and reviewed and commented on the manuscript.

*Corresponding author; e-mail: gnoe@usgs.gov

INTRODUCTION

Hydrologic connectivity with the river channel creates gradients in floodplain hydrology and fluvial geomorphology (hydrogeomorphology) that fundamentally influence ecosystem processes. Inclusion of the four dimensions of hydrologic connectivity, namely, longitudinal, lateral, vertical, and temporal gradients, has improved models of

the ecosystem ecology of river–floodplain systems (Ward 1989; Amoros and Bornette 2002; Stanford and others 2005; Poole 2010; Noe 2013). For example, the lateral exchange of water between river and floodplain, described as the Flood Pulse Concept (Junk and others 1989), is critical to the ability of floodplains to retain watershed water, sediment, and nutrients, and support food webs in riverine landscapes. Hydrologic connectivity and floodplain functions are expected to change laterally as topography and inundation varies across the floodplain (Wharton and others 1982; Junk and others 1989), longitudinally with distance downstream as river discharge and floodplain inundation and width increase (Whigham and others 1988; Brinson 1993; Spink and others 1998), and through time (Stanley and others 1997; Sparks and others 1998). The fluvial geomorphic landforms and processes that permit hydrologic exchange between the channel and the riparian zone promote greater nutrient cycling rates and vegetation production by providing a flood subsidy of resources compared to closed wetland systems (Hopkinson 1992; Heiler and others 1995).

Nitrogen (N) and phosphorus (P) mineralization, the conversion of organic to inorganic forms, is a bottleneck biogeochemical process of ecosystems that influences standing stocks of nutrients and nutrient availability to primary producers. Nutrient mineralization rates in all ecosystems are determined by the abundance of nutrients, the lability of organic matter, and microbial activity (Binkley and Hart 1989). These same factors are thought to control nutrient mineralization rates along gradients of hydrogeomorphology in wetland soils. The quantity and lability of organic matter and nutrients, either input through sedimentation (Adair and others 2004; Wassen and Olde 2006; Kronvang and others 2009; Jolley and others 2010) or stored in soil (Bridgham and others 1998; Spink and others 1998; Verhoeven and others 2001; Wassen and Olde 2006), influence microbial activity and nutrient mineralization in wetlands. Thus, wetland soil nutrient mineralization is impacted by hydrogeomorphic variation, including topography (Burke and others 1999; Wolf and others 2011a), soil texture (Pinay and others 1992; Bechtold and Naiman 2006; McIntyre and others 2009), water table depth and inundation (Hefting and others 2004; Wassen and Olde 2006; Follstad Shah and Dahm 2008; SurrIDGE and others 2007), soil moisture (Adair and others 2004; Sleutel and others 2008), soil redox (Bridgham and others 1998), and earthworm activity (Costello and Lamberti 2009).

The ecosystem theory of floodplains suggests that different geomorphic functional units of varying hydrologic connectivity exist along lateral and longitudinal gradients and their shifting distribution is a function of the dynamic fluvial system (Amoros and others 1987; Ward 1989; Stanford and others 2005). Each of the potential controlling factors for mineralization can vary among geomorphic units arrayed along gradients of connectivity in floodplains (Hupp 2000; Lewis and others 2000; Pinay and others 2000; Johnston and others 2001). Consequently, lateral gradients in floodplain hydrogeomorphology have been shown to influence patterns of other biogeochemical processes, including nutrient sedimentation fluxes (Noe and Hupp 2005), denitrification (Richardson and others 2004; Welti and others 2012), microbial respiration (Welti and others 2012), soil P sorption (Lyons and others 1998; Axt and Walbridge 1999; Bruland and Richardson 2004), and vegetative nutrient fluxes (Clawson and others 2001; Mouw and others 2009). Floodplain productivity and soil nutrient availability increase with river size (Spink and others 1998), and would therefore be expected to change along longitudinal gradients within a watershed. Although these studies have demonstrated meaningful lateral variation in floodplain biogeochemistry, longitudinal variation in floodplain biogeochemistry and the interaction of lateral with longitudinal gradients of hydrologic connectivity have not been well measured as tests of floodplain ecosystem theory.

The goal of this study was to test if soil nutrient mineralization rates varied along longitudinal and lateral geomorphic gradients associated with flood connectivity as predicted by floodplain ecosystem theories. Our objectives were to (1) quantify in situ rates of net N and P mineralization and annual turnover rates of soil nutrients; (2) determine if N and P mineralization changed along longitudinal and lateral floodplain gradients and through time; and (3) identify the hydrogeomorphic controls of N and P mineralization. We predicted that soil N and P mineralization would increase with greater inputs and storage of nutrients and organic matter along spatial gradients of floodplain hydrologic connectivity, and hence be greater at lower elevations along the lateral gradient and at more downstream locations along the longitudinal gradient. Quantification of nutrient mineralization fluxes and controls in floodplain wetlands would benefit efforts to understand the role of floodplains in influencing water quality.

METHODS

Location

We studied the floodplain of Difficult Run, a single channel meandering alluvial river of the Virginia Piedmont, USA, which has three dominant lateral geomorphic units (levee, backswamp, and toe-slope) typical of Piedmont and Coastal Plain floodplains in the eastern US.

Difficult Run is a fifth-order river in the crystalline (gneiss and schist bedrock) Piedmont that is a tributary to the Potomac River and the Chesapeake Bay (Figure 1). Streams and rivers of this region generally have considerable fine-grained deposits of legacy sediment on floodplains and terraces from post-colonial upland erosion. The watershed has a mix of urban, suburban, and forested land use. Mean discharge near the mouth (46 m above NGVD29) of the 151 km² watershed is 1.76 m³ s⁻¹ (US Geological Survey 2007).

Measurements were made in floodplain plots located in each of the three lateral geomorphic units at each of five sites arrayed longitudinally in the watershed. Five floodplain sites were located on the fourth- to fifth-order mainstem of Difficult Run from near the headwaters to the mouth of the watershed (Figure 1). Site locations were chosen to span the watershed, have typical geomorphology and vegetation, and be publicly owned and man-

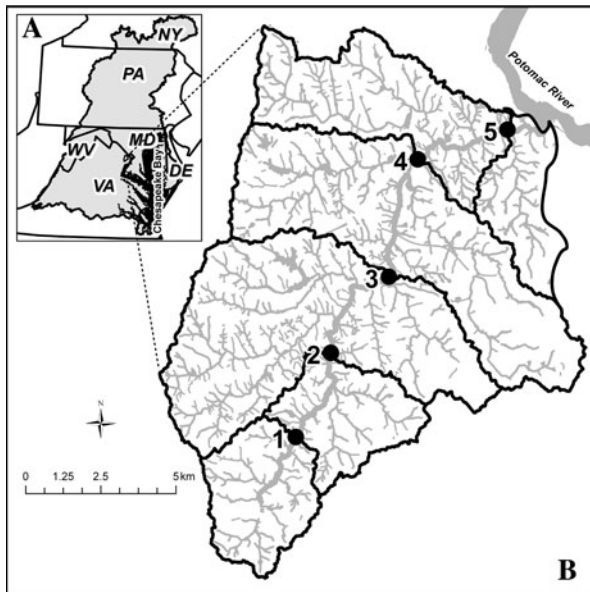


Figure 1. **A** Map showing the location of the Difficult Run watershed in the Chesapeake Bay watershed, USA. **B** Map of the Difficult Run watershed showing the locations and catchment areas of Sites 1–5 in the river network.

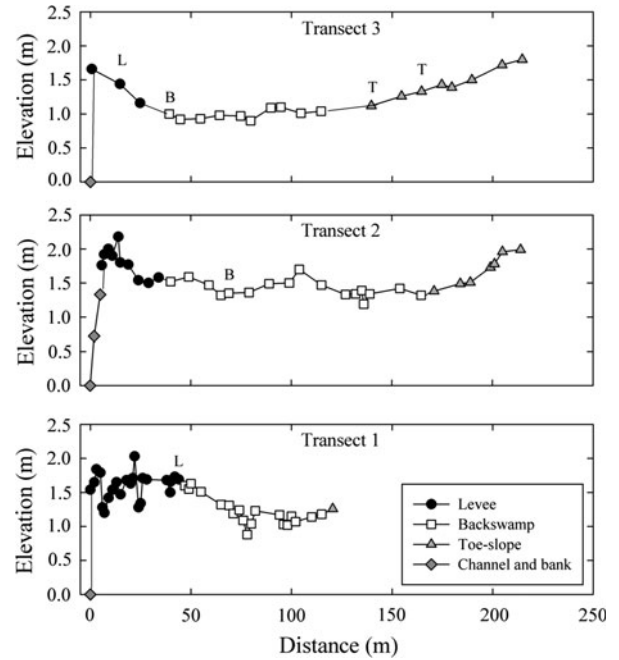


Figure 2. Floodplain soil elevation data relative to river surface water for the three transects at Site 3. The different geomorphic units are shown by *different symbols*, with the location of mineralization plots shown by *letters* above the *symbols* (L levee; B backswamp; T toe-slope).

aged for natural resource protection (Fairfax County Park Authority). Sites 1, 2, 3, 4, and 5 include cumulative catchment areas of 14, 28, 74, 117, and 141 km², respectively. Total floodplain width at each site averaged 80, 65, 160, 160, and 130 m at Sites 1, 2, 3, 4, and 5, respectively. All sites were forested and located on one side of the river.

Each site included three geomorphic units arrayed laterally from channel to uplands: higher elevation natural levee adjacent to the channel, lower elevation backswamp, and higher elevation toe-slope adjacent to the uplands (Figure 2), with the exception of Site 4 that lacked a toe-slope. Each site had three transects oriented perpendicular to the channel that began on the levee near the river and ended at the transition from toe-slope to uplands. Transects were spaced 50 m apart along the longitudinal dimension. Plots were located every 25 m along each transect and classified into one of the three geomorphic units based on site hydrogeomorphic interpretation and relative elevation (Figure 2). From among all the transects within a site, two replicate plots in each geomorphic unit in each site were randomly chosen for measurement of mineralization and ecosystem attributes associated with hydrologic connectivity ($n = 28$ total). All measurements at a plot occurred within 2 m of each other.

Mineralization Measurement

Rates of annual net N and P mineralization in surficial soil were measured in each plot using sequential monthly incubations of modified resin cores for 1 year. Modified resin cores (Noe 2011) use relatively open incubations of intact wetland soil to measure in situ net rates of soil ammonification, nitrification, and P mineralization. The modified resin core design includes three permeable mixed-bed ion-exchange resin bags located above and three resin bags located below soil (0–5 cm depth) incubating inside a 7.8-mm diameter core tube (Figure 3). The resin bags trap NH_4^+ , NO_3^- , and soluble reactive phosphorus (SRP) produced within but transported out of the intact soil core (two inner resin bags adjacent to soil) and prevent external inputs from entering the incubating soil core (two outer resin bags). The two middle bags serve as a quality control check to ensure that the inner and outer bags were not saturated with ions and incapable of trapping nutrients. Modified resin cores allow water and gas exchange and track changes in the surrounding soil abiotic environment, as well as perform better than closed vessel incubations in wetland soils (Noe 2011). Areal net mineralization rates (M) were determined by comparing concentrations in the modified resin cores after field incubation to initial soil cores collected at the start of the incubation.

$$M = \frac{S_r + R_u + R_l - S_i}{AD}$$

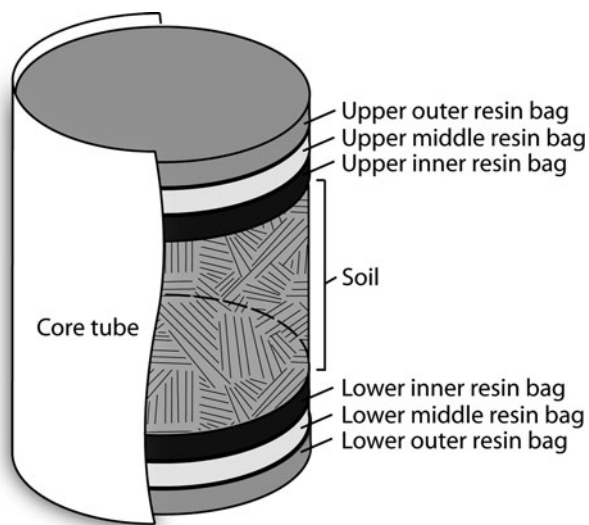


Figure 3. Cutaway diagram of a modified resin core, in which surficial soil (0–5 cm) and six mixed-media ion-exchange resin bags are incubated inside a core tube. Modified from Noe 2011.

where S_r , R_u , R_l , and S_i are the quantity of nutrient (mol) in the soil at the end of the incubation of the modified resin core, resin bag immediately above the soil, resin bag immediately below the soil, and initial soil core, respectively, representing the net production of nutrient, A is the area of the soil core (m^2), and D is the duration of the incubation (days). The production of SRP, NH_4^+ , and NO_3^- estimated net P mineralization, net ammonification, and net nitrification, respectively. Net N mineralization is the sum of ammonification and nitrification, and percent nitrification is calculated as nitrification times 100 divided by net N mineralization. Due to variation in soil bulk density among plots, mineralization rates are expressed on an aerial basis ($\text{mol m}^{-2} \text{ day}^{-1}$). Cumulative annual mineralization is calculated as the sum of mineralization in individual incubations, including negative mineralization rates (immobilization). N and P turnover rates are calculated as the annual mineralization rate divided by the standing stock of TN and TP in the soil ($\text{mol mol}^{-1} \text{ y}^{-1}$, or y^{-1}).

The mineralization sampling area at each plot consisted of a 1 m^2 quadrat that was divided into 100 $10 \times 10\text{-cm}$ cells. At the start of each incubation, an unused cell was randomly chosen for the modified resin core and an adjacent unused cell was randomly chosen for the initial core. Twelve monthly incubations began on September 2, 2008 and ended on September 8, 2009, and the duration of each incubation ranged from 27 to 35 days (average 31 days; total number of incubations in the study 336). A total of 7 modified resin core incubations failed due to thick ice, disappearance, or vandalism. Cumulative annual mineralization rates were calculated only from the duration of successful incubations to account for missing data.

Initial soil cores and modified resin cores were collected from each site in 1 day and stored at 4°C for less than 18 h. Soils from both core types were removed from the core tubes, weighed, and then homogenized with a spatula. A 4-g dw equivalent mass subsample of field moist soil and 2-g ww subsample of resin beads from each of the six resin bags were each placed in a 50-mL centrifuge tube and then extracted with 40 mL of 2 M KCl for 1 h on a 250-rpm shaking table. The samples were then centrifuged at 3000 rpm (soils only) and filtered with a syringe through a $0.2\text{-}\mu\text{m}$ porosity polyethersulfone filter (Pall Corporation, Port Washington, New York USA). Extracts were stored at 4°C until analysis of inorganic nutrients on a segmented flow autoanalyzer (Astoria-Pacific, Astoria, Oregon USA) within 1 week. The 2 M KCl extracts were analyzed for SRP, NO_2^- , NO_3^- , and NH_4^+

(Mulvaney 1996; Reddy and others 1998). Nitrite concentrations were below detection and we report NO_3^- as $\text{NO}_3^- + \text{NO}_2^-$. Every autoanalyzer run included an external reference standard ($\pm 10\%$ of published value QA/QC threshold; ERA, Arvada, Colorado, USA) that was diluted with 2 M KCl and sample blanks (extracts from empty centrifuge tubes or new resin beads in empty centrifuge tubes).

Ecosystem Attributes

A suite of ecosystem attributes were measured that have been shown to vary along gradients of floodplain hydrologic connectivity and to influence nutrient mineralization, including metrics of hydrologic inputs, soil quality, and vegetative inputs (Table 1). Indirect metrics of hydrologic inputs associated with connectivity included plot water level, inundation, sedimentation, and inorganic nutrient loading to the soil surface. A pressure transducer (Esterline Pressure Systems, Hampton, Virginia, USA) was installed in a screened PVC well located adjacent to the lowest elevation plot at each site. Water level was recorded for every 15 min starting in November 2008, after the first two monthly incubations. Mean water elevation and hydroperiod relative to the soil surface (percentage of observations with water depth >0) of each plot at a site was calculated from the transducer water elevation reading and a survey of soil surface at each site using laser levelling. Net sediment accretion at each plot was measured from the change in the depth of sediment over a feldspar clay marker horizon (net deposition) or the exposed length of a buried chain (net erosion) from June 17–27, 2008 to June 22–23, 2009 (Hupp and others, unpublished). Cumulative annual NH_4^+ , NO_3^- , and SRP loading rates to the soil surface were quantified using the accumulation of inorganic nutrients on the upper outer resin bags of the modified resin cores that were flush with the soil surface (Figure 3), representing inputs of inorganic nutrients to the floodplain from floodwater, precipitation, and atmospheric deposition.

A variety of physical, chemical, and biotic attributes of soils were measured. A subsample of soil from each initial core was dried (60°C until constant mass) to estimate water filled pore-space (WFPS; $\{\text{volumetric-moisture} \div [1 - (\text{bulk-density} \div \text{quartz parent material density})]\}$, assuming 2.65 g cm^{-3}) moisture content. Bulk density was estimated from the dry weight equivalent of the soil and the volume of the soil. Ground resin-core soils were each analyzed for TC and TN (CHN

analyzer; Thermo Electron, Milan, Italy), followed by microwave-assisted acid digestion and measurement of total P (ICP-OES; Perkin-Elmer, Waltham, Massachusetts, USA) of the March 2009 incubation only. The remaining soil from initial cores was air dried and then analyzed for pH using a 1:2 soil-to-DI water slurry (Robertson and others 1999). Median particle size (d_{50}) and sand, silt, and clay fractions of mineral (combusted) soil were measured for a single resin core incubation (March 2009) using a LISST-100X laser particle size analyzer (Wolf and others 2011b; Sequoia Scientific, Inc., Bellevue, Washington, USA). Soil temperature was measured by an iButton[®] (15-min sampling frequency; Maxim Integrated Products, Sunnyvale, California, USA) attached mid-depth on the outside of each modified resin core during incubation. Finally, the wet mass of earthworms was measured in each resin core.

Plant litter nutrient inputs were calculated from biomass production at each plot measured using duplicate litterfall traps with monthly collections (elevation 1.2 m above soil surface, surface area 0.3 m^2) and triplicate clip plots of peak herbaceous biomass (1 m^2 ; July 1 to August 10, 2009). The TC, TN, and TP concentrations of plant litter were analyzed similar to soil and used to calculate annual litter nutrient fluxes (Rybicki and others, unpublished data).

Temporal Variation in Sedimentation and Mineralization

The effect of finer scale temporal patterns of sedimentation on mineralization fluxes was tested at a single floodplain location, Site 3, the year prior to the larger study. Five plots were located along a low elevation flowpath, from a crevasse on the natural levee, through the backswamp, and to a depression near a distributary channel that reconnects to the main channel. Three modified resin cores were incubated at each of the five plots for 12 consecutive monthly deployments (for a total of 180 modified resin core incubations) from August 2007 to August 2008. Mineralization rates were reported in Noe (2011).

Sedimentation rate was measured during each incubation using a ceramic tile ($20 \times 20 \text{ cm}$) at each plot. Deposited material, excluding fresh organic detritus (for example, fresh litterfall) without attached mineral sediment, was dried and weighed, ground, and analyzed for TC and TN to calculate mass, C, and N sedimentation fluxes. Mean TP among the plots (0.570 mg g^{-1} ; $n = 5$, one standard error = 0.087), measured from sediment

Table 1. Floodplain Ecosystem Attributes

Measurement	All plots					Longitudinal dimension				
	<i>n</i> = 28	Site 1 <i>n</i> = 6	Site 2 <i>n</i> = 6	Site 3 <i>n</i> = 6	Site 4 <i>n</i> = 4	Site 5 <i>n</i> = 6				
Hydrologic connectivity										
Water elevation above soil surface (m)	-0.90 ± 0.09	-1.12 ± 0.23	-1.12 ± 0.11	-0.95 ± 0.13	-0.38 ± 0.18	-0.75 ± 0.19				
Hydroperiod (days)	16.3 ± 10.7	4.6 ± 4.6	0.5 ± 0.3	0.7 ± 0.3	67.6 ± 66.7	25.3 ± 24.5				
Sediment accretion (mm y ⁻¹)	5.9 ± 2.7	6.2 ± 4.8	8.2 ± 8.2	8.9 ± 3.5	10.3 ± 6.9	-2.8 ± 6.3				
SRP loading to soil surface (mol P m ⁻² y ⁻¹)	9.9 ± 1.0	9.7 ± 1.4	7.0 ± 2.1	12.3 ± 1.6	9.6 ± 2.7	10.8 ± 2.9				
NO ₃ ⁻ loading to soil surface (mol N m ⁻² y ⁻¹)	67 ± 16	54 ± 17	63 ± 24	121 ± 68	58 ± 8	35 ± 6				
NH ₄ ⁺ loading to soil surface (mol N m ⁻² y ⁻¹)	16 ± 2	11 ± 2	9 ± 3	19 ± 2	30 ± 7	15 ± 3				
Soil characteristics										
Soil d50 (µm)	10 ± 0.5	11 ± 0	10 ± 0	10 ± 1	10 ± 2	10 ± 1				
Soil coarse sand (>250 µm, %)	3 ± 1	2 ± 1	3 ± 1	1 ± 0	4 ± 3	5 ± 2				
Soil fine sand (50–250 µm, %)	8 ± 1	8 ± 1	6 ± 1	7 ± 1	9 ± 2	9 ± 2				
Soil silt (2–50 µm, %)	73 ± 1	76 ± 1	75 ± 1	75 ± 1	69 ± 4	70 ± 2				
Soil clay (<2 µm, %)	16 ± 2	14 ± 1	16 ± 1	16 ± 2	18 ± 6	17 ± 2				
Soil bulk density (g cm ⁻³)	0.83 ± 0.02	0.76 ± 0.03	0.87 ± 0.05	0.84 ± 0.03	0.72 ± 0.08	0.94 ± 0.05				
Soil moisture WFPS (%)	65 ± 3	58 ± 6	59 ± 7	67 ± 3	69 ± 13	72 ± 6				
Soil pH	5.61 ± 0.06	5.38 ± 0.23	5.70 ± 0.09	5.68 ± 0.05	5.65 ± 0.07	5.66 ± 0.05				
Soil temperature (°C)	12.1 ± 0.1	12.0 ± 0.1	11.9 ± 0.2	12.3 ± 0.1	12.0 ± 0.1	12.2 ± 0.1				
Soil total C (%)	3.42 ± 0.3	4.2 ± 0.5	3.3 ± 0.7	3.1 ± 0.3	3.9 ± 0.7	2.7 ± 0.5				
Soil total N (%)	0.24 ± 0.02	0.29 ± 0.03	0.24 ± 0.04	0.22 ± 0.03	0.28 ± 0.06	0.21 ± 0.04				
Soil total P (µg g ⁻¹)	491 ± 35	403 ± 86	521 ± 84	495 ± 55	600 ± 130	472 ± 52				
Soil KCl-extractable SRP (µmol P cm ⁻³)	0.0036 ± 0.0004	0.0046 ± 0.0017	0.0028 ± 0.0006	0.0030 ± 0.0004	0.0044 ± 0.0005	0.0032 ± 0.0004				
Soil KCl-extractable NO ₃ ⁻ (µmol N cm ⁻³)	0.16 ± 0.02	0.25 ± 0.05	0.06 ± 0.03	0.22 ± 0.06	0.09 ± 0.02	0.18 ± 0.02				
Soil KCl-extractable NH ₄ ⁺ (µmol N cm ⁻³)	0.12 ± 0.01	0.14 ± 0.03	0.09 ± 0.02	0.11 ± 0.01	0.21 ± 0.05	0.09 ± 0.02				
Soil worm mass (g ww m ⁻²)	4.8 ± 1.5	1.5 ± 1.2	4.4 ± 2.6	10.3 ± 4.9	1.5 ± 1.1	5.4 ± 3.6				
Vegetative inputs										
Litterfall C flux (mg C m ⁻² d ⁻¹)	628 ± 24	708 ± 43	571 ± 34	618 ± 45	583 ± 86	643 ± 67				
Litterfall N flux (mg N m ⁻² d ⁻¹)	17.5 ± 0.9	16.5 ± 0.5	12.1 ± 1.2	19.6 ± 1.7	19.7 ± 2.9	20.2 ± 1.7				
Litterfall P flux (mg P m ⁻² d ⁻¹)	1.56 ± 0.07	1.56 ± 0.09	1.13 ± 0.08	1.63 ± 0.16	1.79 ± 0.23	1.76 ± 0.16				
Herbaceous C flux (mg C m ⁻² d ⁻¹)	38.7 ± 8.4	15.1 ± 4.1	10.6 ± 5.5	83.6 ± 20.6	82.0 ± 26.1	16.5 ± 2.9				
Herbaceous N flux (mg N m ⁻² d ⁻¹)	1.89 ± 0.36	0.79 ± 0.18	0.57 ± 0.31	4.01 ± 0.81	3.74 ± 0.97	0.98 ± 0.16				
Herbaceous P flux (mg P m ⁻² d ⁻¹)	0.186 ± 0.038	0.080 ± 0.019	0.055 ± 0.031	0.398 ± 0.094	0.370 ± 0.119	0.089 ± 0.019				

Table 1. continued

Measurement	Lateral dimension		
	Levee <i>n</i> = 10	Backswamp <i>n</i> = 10	Toe-slope <i>n</i> = 8
Hydrologic connectivity			
Water elevation above soil surface (m)	-0.93 ± 0.12	-0.67 ± 0.16	-1.15 ± 0.15
Hydroperiod (days)	0.5 ± 0.3	44.8 ± 32.1	0.5 ± 0.2
Sediment accretion (mm y ⁻¹)	14.9 ± 5.1	0.2 ± 4.9	1.7 ± 1.0
SRP loading to soil surface (mol P m ⁻² y ⁻¹)	8.7 ± 1.5	9.2 ± 1.7	12.3 ± 1.7
NO ₃ ⁻ loading to soil surface (mol N m ⁻² y ⁻¹)	39 ± 6	67 ± 14	100 ± 53
NH ₄ ⁺ loading to soil surface (mol N m ⁻² y ⁻¹)	12 ± 2	20 ± 4	15 ± 2
Soil characteristics			
Soil d50 (µm)	11 ± 0	10 ± 1	10 ± 0
Soil coarse sand (>250 µm, %)	3 ± 1	2 ± 1	4 ± 1
Soil fine sand (50–250 µm, %)	7 ± 1	9 ± 2	7 ± 1
Soil silt (2–50 µm, %)	76 ± 1	71 ± 2	72 ± 1
Soil clay (<2 µm, %)	14 ± 1	18 ± 3	17 ± 1
Soil bulk density (g cm ⁻³)	0.87 ± 0.03	0.83 ± 0.06	0.79 ± 0.03
Soil moisture WFPS (%)	53 ± 4	75 ± 5	67 ± 5
Soil pH	5.79 ± 0.04	5.62 ± 0.04	5.37 ± 0.14
Soil temperature (°C)	12.2 ± 0.1	12.0 ± 0.1	12.0 ± 0.1
Soil total C (%)	2.8 ± 0.3	3.4 ± 0.6	4.3 ± 0.3
Soil total N (%)	0.20 ± 0.02	0.24 ± 0.04	0.30 ± 0.02
Soil total P (µg g ⁻¹)	362 ± 38	509 ± 66	630 ± 44
Soil KCl-extractable SRP (µmol P cm ⁻³)	0.0030 ± 0.0005	0.0029 ± 0.0004	0.0052 ± 0.0010
Soil KCl-extractable NO ₃ ⁻ (µmol N cm ⁻³)	0.13 ± 0.02	0.17 ± 0.05	0.19 ± 0.05
Soil KCl-extractable NH ₄ ⁺ (µmol N cm ⁻³)	0.10 ± 0.02	0.13 ± 0.03	0.14 ± 0.02
Soil worm mass (g ww m ⁻²)	4.1 ± 2.1	2.4 ± 1.4	8.8 ± 4.0
Vegetative inputs			
Litterfall C flux (mg C m ⁻² d ⁻¹)	687 ± 46	579 ± 41	615 ± 32
Litterfall N flux (mg N m ⁻² d ⁻¹)	19.0 ± 2.0	16.4 ± 1.6	17.0 ± 0.6
Litterfall P flux (mg P m ⁻² d ⁻¹)	1.66 ± 0.16	1.45 ± 0.13	1.56 ± 0.08
Herbaceous C flux (mg C m ⁻² d ⁻¹)	38.2 ± 15.3	48.2 ± 18.0	27.2 ± 9.9
Herbaceous N flux (mg N m ⁻² d ⁻¹)	1.91 ± 0.68	2.24 ± 0.74	1.45 ± 0.46
Herbaceous P flux (mg P m ⁻² d ⁻¹)	0.177 ± 0.068	0.232 ± 0.083	0.141 ± 0.047

Annual mean (±1SE) values of floodplain ecosystem attributes are presented for all plots, for each longitudinal site, and for each lateral geomorphic feature. Sites are numbered with increasing distance downstream. Site 4 does not have a toe-slope.

n = sample size; d50 = median particle size; WFPS = water-filled pore space; SRP = soluble reactive P.

accumulated on marker horizons in a pilot study, was used to estimate P sedimentation flux.

Statistics

Longitudinal, lateral, and temporal differences in monthly mineralization rates were tested using repeated measures analysis of variance (RM-ANOVA; SAS 9.1), with longitudinal and lateral positions as the main factors and time as the repeated measure. The RM-ANOVA models included two-way interaction terms; models with a three-way interaction term underperformed the simpler model based on Akaike Information Criteria indices. Significant lateral or longitudinal terms in the RM-ANOVA models were further evaluated using Tukey's post hoc tests. Because of the unbalanced experimental design caused by the lack of toe-slope at Site 4, a second set of RM-ANOVA models with post hoc tests was analyzed with Site 4 omitted to compare the toe-slope to the levee and backswamp geomorphic units. Associations between annual mineralization rates and each of the individual ecosystem attributes were tested using Pearson product-moment correlation analyses. All variables were evaluated for normality and transformed appropriately when necessary. All statistical tests were evaluated using $\alpha = 0.05$.

RESULTS

Lateral and Longitudinal Differences in Soil Mineralization Rates

Mineralization rates differed among floodplain geomorphic units for net ammonification, net nitrification, percent nitrification, net N mineralization, and net P mineralization (RM-ANOVAs, Table 2). Ammonification and P mineralization were both much greater in the backswamp than the levee, whereas nitrification and percent nitrification were both much greater in the levee than the backswamp (Table 2). Net N mineralization rates, the sum of ammonification and nitrification, did not differ between levee and backswamp because of the balancing opposite effects of the two constituent processes. However, net N mineralization was greater in the toe-slope than either the levee or backswamp. Otherwise, the toe-slope was similar to either levee or backswamp for the other mineralization rates. Notably, N and P turnover (the amount mineralized relative to the soil pool) did not change laterally across the floodplain. Lateral differences in geomorphology also interacted with the time of incubation to affect ammonification, with both backswamp and toe-slope, but not

the levee, having elevated ammonification during Spring when soils were the wettest compared to the rest of the year.

Few significant differences in floodplain mineralization rates were identified longitudinally through the watershed. Site effects were significant for only ammonification and nitrification, with greater nitrification at Sites 1 and 3 compared to Site 2 and a pattern of enhanced ammonification at Sites 3 and 4 (Table 2). The effect of lateral geomorphic units also depended on longitudinal site position, as indicated by their significant interaction for ammonification and nitrification. Specifically, ammonification rates were the highest in the wet backswamp at Site 4 and nitrification rates were higher in the backswamp than the levee and toe-slope at Site 2. The longitudinal effect of site also interacted with the time of incubation to affect P mineralization indicating that sites had unique temporal patterns.

Mineralization rates varied among the monthly incubations of the year-long study. Ammonification, nitrification, net N mineralization, P mineralization, N turnover, and P turnover all significantly varied over time in the repeated measures ANOVAs, but percent nitrification did not (Table 2). Thus, there was substantial seasonal variation in mineralization rates. Mineralization rates, for net N in particular, were lower in the colder winter months and higher in the warmer late spring and summer months (data not shown).

Longitudinal and Lateral Gradients in Ecosystem Hydrologic Inputs, Soils, and Vegetation

Headwater floodplain soils tended to be more organic with greater nutrient content and lower bulk density than downstream floodplain soils (Table 1). In contrast, downstream floodplains had greater hydrologic connectivity (shallower ground water depth, wetter soils, longer hydroperiod, and greater inorganic nutrient loading to the soil surface) and greater vegetative inputs (litterfall fluxes and herbaceous production) than the headwater floodplains.

The natural levees adjacent to the river channel occurred at relatively high elevations and thus had less hydrologic connection (inundated less often, deeper groundwater, less soil moisture, and less inorganic nutrient loading to the soil surface) than the low elevation backswamps, whereas the toe-slope geomorphic unit, adjacent to uplands, typically had intermediate wetness (Table 1). Soil texture did not change along lateral or longitudinal

Table 2. Soil Annual Nutrient Mineralization Rates

	<i>n</i>	Ammonification (mmol N m ⁻² y ⁻¹)	Nitrification (mmol N m ⁻² y ⁻¹)	Net N mineralization (mmol N m ⁻² y ⁻¹)	% nitrification	P mineralization (mmol P m ⁻² y ⁻¹)	N turnover (y ⁻¹)	P turnover (y ⁻¹)
All plots	329	127 ± 33	192 ± 26	319 ± 35	66 ± 7	3.60 ± 0.41	0.044 ± 0.004	0.0026 ± 0.0003
Longitudinal								
Site 1	72	66 ± 34	251 ± 55a	317 ± 50	81 ± 13	3.61 ± 0.91	0.041 ± 0.006	0.0036 ± 0.0008
Site 2	72	111 ± 45	111 ± 50b	221 ± 41	51 ± 16	3.85 ± 1.61	0.032 ± 0.004	0.0029 ± 0.0014
Site 3	68	167 ± 88	258 ± 59a	425 ± 109	75 ± 15	3.61 ± 0.51	0.053 ± 0.009	0.0022 ± 0.0002
Site 4	47	258 ± 168	163 ± 81	421 ± 114	54 ± 28	3.52 ± 0.93	0.063 ± 0.014	0.0023 ± 0.0003
Site 5	70	77 ± 34	168 ± 47	245 ± 46	65 ± 11	3.36 ± 0.47	0.034 ± 0.004	0.0020 ± 0.0002
Lateral								
Levee	120	12 ± 13a	222 ± 34a	234 ± 29a	94 ± 6a	2.18 ± 0.19a	0.041 ± 0.006	0.0021 ± 0.0002
Backswamp	116	203 ± 68b	144 ± 49b	347 ± 82a	47 ± 12b	4.19 ± 0.53b	0.045 ± 0.008	0.0029 ± 0.0005
Toe-slope	93	176 ± 56b	214 ± 52ab	390 ± 44b	54 ± 11ab	4.62 ± 1.10ab	0.045 ± 0.005	0.0029 ± 0.0010
Repeated measures ANOVA <i>P</i> values								
Time		<0.0001	<0.0001	<0.0001	0.719	<0.0001	<0.0001	0.032
Lateral		<0.0001	0.036	0.015	0.036	0.013	0.688	0.162
Longitudinal		<0.0001	0.028	0.278	0.230	0.996	0.179	0.847
Lateral * longitudinal		<0.0001	0.034	0.659	0.383	0.605	0.657	0.228
Longitudinal * time		0.054	0.410	0.448	0.717	0.044	0.431	0.211
Lateral * time		<0.0001	0.983	0.103	0.221	0.959	0.077	0.890

Annual mineralization rates (average ± 1SE) are presented for all plots, for each longitudinal site, and for each lateral geomorphic feature. Sites are numbered with increasing distance downstream. Different letters next to mineralization rates indicate significant differences among longitudinal or among lateral gradients as determined by Tukey post hoc tests. *P* values are provided for repeated measures ANOVA performed on monthly incubation data. Bold *P* values <0.05; italicized *P* values <0.10. Site 4 does not have a toe-slope.
n = sample size.

gradients in the floodplain. Levees had much greater rates of sediment deposition than the backswamp. Finally, soil TP and SRP contents were greater and pH lower in soils of the toe-slope than either backswamp or levee.

Ecosystem Controls of Annual Soil Mineralization Rates

Annual net mineralization rates of P and N generally covaried (Table 3). P mineralization rates increased with ammonification (Pearson product-moment correlation, $n = 28$, $r = 0.654$, $P < 0.001$) and net N mineralization rates ($r = 0.384$, $P = 0.044$) and decreased with percent nitrification ($r = -0.566$, $P = 0.002$). Ammonification and nitrification were negatively associated ($r = -0.433$, $P = 0.021$).

Annual net ammonification rate increased with ecosystem attributes indicating greater hydrologic connectivity and wetness and finer texture soils with more nutrient content. Ammonification was positively correlated with hydroperiod, ammonium loading to the soil surface, soil WFPS, soil TN, soil TP, and soil percent clay, and negatively correlated with soil percent silt and soil d50 (Table 3). Of these ecosystem hydrogeomorphic attributes, soil WFPS had the strongest relationship ($r = 0.577$) with ammonification.

Annual net nitrification rate had significant correlations with only a few ecosystem attributes. Nitrification rate increased weakly with the soil stoichiometric ratios of soil C:P, soil C:N, and soil N:P (Table 3). However, percent nitrification decreased with greater wetness and finer textured soils. Percent nitrification decreased with hydroperiod, soil WFPS, soil percent clay, and soil TP, and increased with soil percent silt, sediment accretion, and soil temperature (Table 3). Of these ecosystem hydrogeomorphic attributes, soil WFPS had the strongest relationship with percent nitrification ($r = -0.563$, Figure 4); in other words, wetter soils had a smaller proportion of DIN production as nitrate.

Annual net N mineralization rate was correlated with many individual ecosystem variables associated with hydrologic connectivity, soil organic and nutrient content, and vegetation inputs. N mineralization increased with ammonium loading to the soil surface, soil TN and TC and TP and N:P and C:P, soil KCl-extractable NH_4^+ and SRP, and herbaceous litter P and C and N production, and decreased with soil bulk density (Table 3). Soil TN was most strongly correlated with net N mineralization ($r = 0.677$, Figure 4).

Annual net P mineralization rate varied with gradients of hydrologic connectivity and soil characteristics. P mineralization had the strongest correlation with and increased with ammonium loading to the soil surface ($r = 0.539$, Figure 4), and also increased with SRP loading to the soil surface, and decreased with soil percent silt, soil pH, and annual sediment accretion (Table 3).

N turnover rate increased with ammonium loading to the soil surface ($r = 0.652$), herbaceous litter C (Figure 4) and P and N production and soil KCl-extractable NH_4^+ and SRP, and decreased with soil bulk density (Table 3). P turnover rate increased with soil C:P ($r = 0.388$, Figure 4) and N:P, and SRP loading to the soil surface (Table 3).

Effect of Sedimentation on Monthly Mineralization Rates

The influence of sedimentation on monthly soil nutrient mineralization was evaluated by comparing individual mineralization incubations with concurrent sediment deposition on tiles at five plots along a floodplain flowpath at Site 3. More monthly sediment deposition led to higher monthly nutrient mineralization rates. Net N mineralization rate increased with the amount of N sedimentation (Figure 5; Pearson product-moment correlation, $n = 60$, $r = 0.295$, $P = 0.022$) as well as the amount of mass and C sedimentation during each incubation ($r > 0.265$, $P < 0.041$). P mineralization rate also increased with the mass of sediment deposition (Figure 5; $r = 0.508$, $P < 0.001$) and the amount of C and N sedimentation during each incubation ($r > 0.450$, $P < 0.001$). Unlike net N mineralization, P mineralization rate increased both with the amount of mass, C, and N sedimentation during the incubation as well as the amount immediately prior to the incubation ($r > 0.380$, $P < 0.004$). Although sedimentation stimulated mineralization, the amount of N or P mineralized in the soil during incubation was substantially less than the amount of N or P deposited with sedimentation (Figure 5). The mass-weighted average C and N contents of the deposited sediment among all plots was 10.7 and 0.41%, respectively. The average P content of sediment deposited over marker horizons at all Difficult Run sites is $518 \mu\text{g g}^{-1}$ (Noe 2013). Thus, newly deposited sediment was enriched in C and N, but not P, compared to surficial soil (Table 1). Cumulative annual sedimentation rates ranged from 1,124- to 8,187-g dw $\text{m}^{-2} \text{y}^{-1}$ among the five floodplain flowpath plots at Site 3 (mean: $3,917 \text{ g m}^{-2} \text{y}^{-1}$).

Table 3. Correlations Between Mineralization Rates and Ecosystem Attribute Variables

Ecosystem attributes	Statistic	Ammonification	Nitrification	% Nitrification	Nitrification	N mineralization	N turnover	P mineralization	P turnover
Mineralization									
Nitrification (mol N m ⁻² y ⁻¹)	r	-0.433							
	P	0.021							
% nitrification	r	-0.879	0.702						
	P	0.000	0.000						
N mineralization (mol N m ⁻² y ⁻¹)	r	0.540	0.449	-0.248					
	P	0.003	0.016	0.203					
N turnover (mol N mol N ⁻¹ y ⁻¹)	r	0.451	0.420	-0.163	0.862				
	P	0.016	0.026	0.408	0.000				
P mineralization (mol P m ⁻² y ⁻¹)	r	0.654	-0.249	-0.566	0.384	0.310			
	P	0.000	0.202	0.002	0.044	0.109			
P turnover (mol P mol P ⁻¹ y ⁻¹)	r	0.357	-0.126	-0.236	0.223	0.251	0.764		
	P	0.063	0.522	0.227	0.254	0.197	0.000		
Hydrologic connectivity									
Water elevation above soil surface (m)	r	0.348	-0.261	-0.312	0.093	0.126	-0.019	0.015	
	P	0.069	0.180	0.106	0.638	0.524	0.923	0.941	
Hydroperiod (days)	r	0.473	-0.252	-0.434	0.225	0.227	0.252	0.038	
	P	0.011	0.197	0.021	0.250	0.245	0.195	0.846	
Sediment accretion (mm y ⁻¹)	r	-0.343	0.163	0.442	-0.191	0.091	-0.434	-0.049	
	P	0.074	0.408	0.019	0.330	0.645	0.021	0.806	
NH ₄ ⁺ loading to soil surface (mol N m ⁻² y ⁻¹)	r	0.448	0.056	-0.305	0.591	0.652	0.539	0.319	
	P	0.017	0.779	0.115	0.001	0.000	0.003	0.098	
NO ₃ ⁻ loading to soil surface (mol N m ⁻² y ⁻¹)	r	0.237	-0.029	-0.212	0.140	0.166	0.137	-0.071	
	P	0.225	0.883	0.279	0.479	0.398	0.487	0.719	
SRP loading to soil surface (mol P m ⁻² y ⁻¹)	r	0.045	0.262	0.117	0.229	0.149	0.486	0.346	
	P	0.822	0.179	0.555	0.242	0.448	0.009	0.071	
Soil characteristics									
Soil d50 (µm)	r	-0.473	0.142	0.347	-0.269	-0.227	-0.265	-0.184	
	P	0.011	0.470	0.071	0.167	0.245	0.173	0.349	
Soil coarse sand (>250 µm, %)	r	-0.147	-0.113	0.111	-0.267	-0.158	0.179	0.215	
	P	0.456	0.566	0.575	0.170	0.422	0.363	0.272	
Soil fine sand (50–250 µm, %)	r	-0.177	0.191	0.090	0.118	0.033	-0.126	-0.285	
	P	0.369	0.330	0.649	0.551	0.869	0.523	0.142	
Soil silt (2–25 µm, %)	r	-0.478	0.192	0.498	-0.338	-0.355	-0.467	-0.175	
	P	0.010	0.327	0.007	0.079	0.064	0.012	0.373	
Soil clay (<2 µm, %)	r	0.546	-0.101	-0.433	0.372	0.283	0.298	0.091	
	P	0.003	0.610	0.021	0.051	0.144	0.123	0.646	
Soil bulk density (g cm ⁻³)	r	-0.254	-0.290	0.024	-0.636	-0.426	-0.257	-0.247	
	P	0.192	0.135	0.905	0.000	0.024	0.187	0.205	
Soil moisture WFPS (%)	r	0.577	-0.266	-0.563	0.322	0.131	0.316	-0.066	
	P	0.001	0.172	0.002	0.095	0.507	0.101	0.739	

Table 3. continued

Ecosystem attributes	Statistic	Ammonification	Nitrification	% Nitrification	N mineralization	N turnover	P mineralization	P turnover
Soil pH	<i>r</i>	-0.109	-0.195	0.047	-0.336	-0.177	-0.445	-0.220
	<i>P</i>	0.581	0.320	0.814	0.080	0.367	0.018	0.262
Soil temperature (°C)	<i>r</i>	-0.241	0.251	0.376	-0.106	0.080	-0.280	-0.199
	<i>P</i>	0.217	0.197	0.049	0.591	0.686	0.149	0.311
Soil total C (%)	<i>r</i>	0.302	0.306	-0.094	0.652	0.270	0.297	0.184
	<i>P</i>	0.118	0.113	0.634	0.000	0.165	0.125	0.350
Soil total N (%)	<i>r</i>	0.397	0.239	-0.196	0.677	0.263	0.318	0.141
	<i>P</i>	0.036	0.220	0.319	0.000	0.177	0.100	0.475
Soil total P (µg g ⁻¹)	<i>r</i>	0.521	-0.058	-0.430	0.476	0.270	0.314	-0.267
	<i>P</i>	0.004	0.771	0.022	0.010	0.165	0.103	0.169
Soil C:N	<i>r</i>	-0.253	0.392	0.353	0.185	0.177	-0.027	0.183
	<i>P</i>	0.194	0.039	0.066	0.346	0.367	0.892	0.351
Soil C:P	<i>r</i>	-0.041	0.420	0.194	0.396	0.168	0.046	0.388
	<i>P</i>	0.835	0.026	0.322	0.037	0.393	0.816	0.041
Soil N:P	<i>r</i>	0.036	0.382	0.120	0.426	0.141	0.080	0.388
	<i>P</i>	0.856	0.045	0.543	0.024	0.473	0.687	0.041
Soil KCl-extractable NH ₄ ⁺ (mol N cm ⁻³)	<i>r</i>	0.142	0.309	0.068	0.562	0.442	0.327	0.272
	<i>P</i>	0.473	0.110	0.731	0.002	0.019	0.089	0.161
Soil KCl-extractable NO ₃ ⁻ (mol N cm ⁻³)	<i>r</i>	-0.324	0.282	0.368	-0.104	-0.037	-0.175	-0.141
	<i>P</i>	0.092	0.146	0.054	0.598	0.851	0.372	0.475
Soil KCl-extractable SRP (mol P cm ⁻³)	<i>r</i>	0.136	0.363	-0.009	0.532	0.426	0.204	0.062
	<i>P</i>	0.490	0.057	0.966	0.004	0.024	0.299	0.754
Soil worm mass (g ww m ⁻²)	<i>r</i>	0.053	0.196	0.064	0.185	0.021	-0.218	-0.307
	<i>P</i>	0.787	0.318	0.746	0.345	0.914	0.265	0.112
Vegetative inputs								
Litterfall C flux (mol C m ⁻² y ⁻¹)	<i>r</i>	-0.126	0.165	0.153	-0.046	-0.068	-0.195	0.066
	<i>P</i>	0.523	0.401	0.438	0.817	0.731	0.321	0.740
Litterfall N flux (mol N m ⁻² y ⁻¹)	<i>r</i>	-0.049	0.302	0.156	0.189	0.252	-0.001	-0.021
	<i>P</i>	0.806	0.118	0.429	0.335	0.195	0.997	0.914
Litterfall P flux (mol P m ⁻² y ⁻¹)	<i>r</i>	0.098	0.239	-0.009	0.276	0.284	-0.013	-0.055
	<i>P</i>	0.621	0.220	0.962	0.155	0.143	0.946	0.781
Herbaceous C flux (mol C m ⁻² y ⁻¹)	<i>r</i>	0.202	0.200	-0.012	0.408	0.540	-0.038	-0.116
	<i>P</i>	0.303	0.309	0.952	0.031	0.003	0.849	0.555
Herbaceous N flux (mol N m ⁻² y ⁻¹)	<i>r</i>	0.135	0.242	0.047	0.374	0.516	-0.078	-0.155
	<i>P</i>	0.493	0.216	0.813	0.050	0.005	0.693	0.431
Herbaceous P flux (mol P m ⁻² y ⁻¹)	<i>r</i>	0.194	0.235	0.004	0.418	0.533	-0.028	-0.130
	<i>P</i>	0.324	0.229	0.982	0.027	0.004	0.886	0.510

Significant correlations ($P < 0.05$) are bold.
d50 = median particle size; WFPS = water-filled pore space; SRP = soluble reactive P.

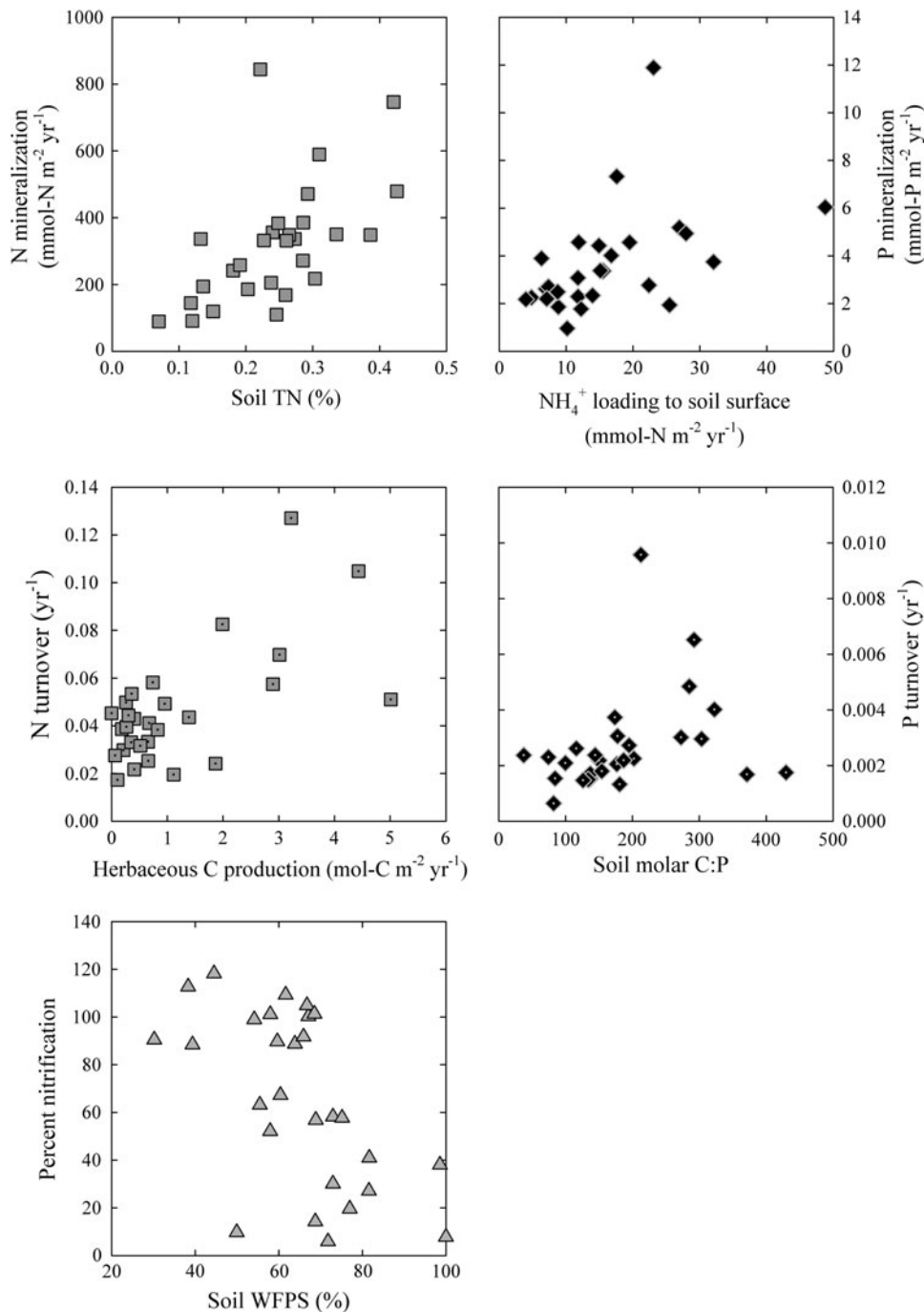


Figure 4. Relationships between cumulative annual mineralization rates and their most correlated ecosystem attributes. *WFPS* water-filled pore space.

Turnover of Soil N and P Pools

The cumulative annual net nutrient mineralization rates were divided by the standing stocks of total nutrients in the plots to calculate the turnover rates of soil N and P pools. Annual turnover of soil N averaged $0.046 \pm 0.005 \text{ yr}^{-1}$ ($\pm 1\text{SE}$), or 22 years to mineralize the existing pool of soil TN. In contrast, the average annual turnover rate of soil P was $0.0027 \pm 0.0003 \text{ yr}^{-1}$, or 369 years to mineralize the existing standing stock of soil TP. Both estimates of

nutrient depletion times assume no new inputs of N and P, although nutrient inputs to the floodplain likely occur from both riparian transport from adjacent uplands and floodplain transport (overbank flow) from upstream catchment, as well as floodplain litter production.

DISCUSSION

Hydrologic connectivity with the river channel creates gradients in floodplain hydrogeomorphology

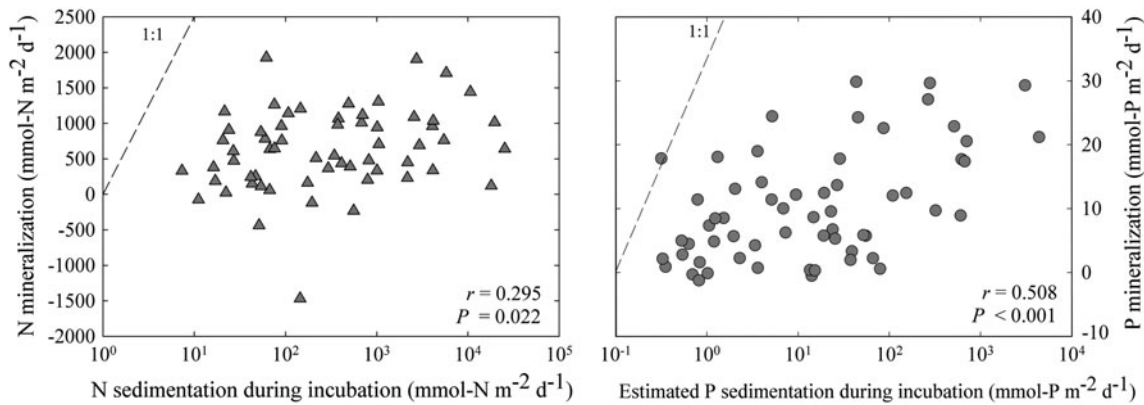


Figure 5. Net N and P mineralization rates compared to N and P sedimentation rates during each deployment. The 1:1 line between mineralization and sedimentation fluxes is shown as a *dashed line*.

that fundamentally influence ecosystem processes (Amoros and others 1987; Junk and others 1989; Ward 1989; Amoros and Bornette 2002; Stanford and others 2005; Poole 2010; Noe 2013). Floodplains ecosystem theory suggests that different geomorphic functional units of varying hydrologic connectivity exist along lateral and longitudinal gradients and their shifting distribution is a function of the dynamic fluvial system (Amoros and others 1987; Ward 1989; Stanford and others 2005). This mosaic of floodplain ecosystem hydrologic connectivity should lead to strong spatial gradients in soil N and P mineralization by influencing the factors known to influence mineralization, namely, organic nutrient quantity and lability and microbial activity.

Landscape Variation in Floodplain Mineralization

Floodplain soil nutrient mineralization varied mostly laterally but also somewhat longitudinally in the Difficult Run watershed. Only ammonification and nitrification rates differed longitudinally among sites, and P mineralization varied among sites depending on the time of year. There are few examples of longitudinal variation in floodplain biogeochemistry in the literature. Lockaby and others (2005) found significant differences in microbial biomass C and N, but not N mineralization, between riparian plots located in upper versus lower watershed locations but only when there were strong longitudinal differences in sedimentation. Floodplain nutrient sedimentation fluxes also vary with sedimentation rates along the longitudinal gradient of rivers (Noe and Hupp 2005).

All measured N and P mineralization fluxes, as well as percent nitrification, differed laterally among geomorphic units. Many studies have found

lateral variation in floodplain biogeochemistry, including nutrient sedimentation (Steiger and Gurnell 2002; Kroes and others 2007; Kronvang and others 2009), denitrification (Richardson and others 2004; Olde Venterink and others 2006), and P sorption (Lyons and others 1998; Axt and Walbridge 1999). N mineralization potential (lab incubations, Bechtold and Naiman 2006; McIntyre and others 2009) and in situ N mineralization fluxes using closed vessel incubation (Van Cleve and others 1993; Burke and others 1999; Wassen and others 2002) also has been shown to change laterally across floodplain geomorphic units, but not always (Adair and others 2004). One other study investigated and found lateral variation in floodplain P mineralization, with a peak in soil P release in the middle of the floodplain (Wassen and others 2002).

Controls of Floodplain Mineralization

The lateral and longitudinal variability of nutrient mineralization fluxes was associated with spatial gradients of hydrologic connectivity in the floodplains. The floodplain ecosystem attributes that were predictive of mineralization can be generally classified as sediment and inorganic nutrient inputs, quantity and lability of soil nutrients and vegetative inputs, and soil moisture and oxidation state, and showed clear lateral and longitudinal gradients associated with hydrologic connectivity. Headwater floodplain soils were more organic with greater nutrient content, whereas downstream floodplains had greater hydrologic connectivity. The longitudinal hydrologic gradient is typical of floodplains (Junk and others 1989). The natural levees adjacent to the river channel occurred at relatively high elevations and thus had less hydrologic connection than the low elevation

backswamps, whereas the toe-slope geomorphic unit, adjacent to uplands, typically had intermediate wetness. The basic control of relative elevation on inundation dynamics and soil moisture in floodplains is common (Hupp 2000; Johnston and others 2001; Stoeckel and Miller-Goodman 2001; Hupp and others 2008). Surprisingly, soil texture did not change along lateral or longitudinal gradients in the floodplain, even though others have found coarser soil texture on levees and lower in watersheds (Pizzuto 1987; Hupp 2000; Petts and others 2000). Levees had much greater rates of sediment deposition than the backswamp, in this study, and at many more floodplain locations in Difficult Run (Hupp and others, unpublished). This lateral gradient of mineral sediment input also was evident in the gradient of increasing soil organic and N content from levee to backswamp to toe-slope.

Sediment and Nutrient Inputs from Flooding

Areas of the floodplain with a longer hydroperiod had greater ammonium loading rates to the soil surface, which typically was found in the backswamp geomorphic unit lower in the watershed. Thus, locations with greater ammonium loading rates can be inferred to have greater ammonium inputs from flooding in this small watershed with relatively homogenous forest structure, as opposed to greater ammonium loading from precipitation or atmospheric inputs. Soil ammonification, net N mineralization, N turnover, and P mineralization all increased with enhanced loading of ammonium to the soil surface, suggesting that flood subsidy of inorganic N was associated with greater soil nutrient mineralization rates. Floodplain locations with greater SRP loading to the soil surface also had greater P mineralization and turnover, but because SRP loading was unrelated to hydroperiod, this cannot be directly attributed to hydrologic connectivity gradients.

Spatial and temporal patterns of mineralization along a low elevation flowpath at one of our sites, located mid-watershed, showed a positive association between monthly floodplain sedimentation and nutrient mineralization. The newly deposited sediment was finely textured and had greater TC and TN than the surficial soil. Thus, sediment deposited at this site is richer in nutrients and represents a nutrient subsidy to floodplain soil that fueled nutrient mineralization. Others have also found that sedimentation inputs can increase nutrient mineralization rates in floodplains (Adair and others 2004; Wassen and Olde 2006; Kronvang

and others 2009). In contrast, Jolley and others (2010) measured decreases in riparian soil N mineralization potential and microbial C and N in sites with sedimentation of coarse, sandy material greater than between 0.1 and 0.4 cm y^{-1} . Annual sediment accretion rates in this study were similar to those of Jolley and others (2010); throughout the watershed, floodplain accretion rates averaged 0.6 cm y^{-1} , ranging from 0.02 cm y^{-1} in backswamps to 1.49 cm y^{-1} in levees. At the single mid-watershed site, mass sedimentation rates converted to vertical accretion rates using underlying surficial soil bulk density range from 0.13 to 1.04 cm y^{-1} . Thus, the size fractionation and biogeochemical characteristics of deposited sediment clearly influences its effects on riparian ecosystem processes.

However, we also found conflicting spatial associations between annual floodplain sedimentation and soil nutrient mineralization rates when analyzed at the larger spatial scale that included all five sites and greater sampling of levees. Spatial patterns of net sedimentation throughout the watershed were negatively correlated with P mineralization and positively correlated with percent nitrification. These patterns are likely an artifact of the highest sedimentation rates occurring at the shortest hydroperiods on the levees (Hupp and others, unpublished). The levees had much higher net sedimentation rates than backswamps, which were sometimes net erosional. The higher and drier levees also had lower nutrient mineralization rates due to lower soil moisture and organic content, and greater nitrification of ammonium to nitrate due to more oxygenated soils, compared to both backswamp and toe-slope.

Soil Moisture and Oxidation State

Mineralization rates also were influenced by soil moisture and oxidation state. Sleutel and others (2008) found that N mineralization potential in wetland soils peaks at intermediate levels of water-filled pore space (WFPS), 65%, decreasing below this threshold due to moisture limitation and above this threshold due to reduced oxygen availability. We did not measure soil oxidation state directly, instead, we use soil WFPS as a proxy for oxygen availability. Spatial patterns of ammonification, net N mineralization, and P mineralization increased linearly with soil moisture, and did not have a unimodal distribution in contrast to Sleutel and others (2008). These findings suggest that moisture limitation was more important to net N and P mineralization than oxygen limitation even in the

wettest soils, in contrast to other studies that found N mineralization decreased in wetter and anaerobic soils (Bridgham and others 1998; Wassen and Olde 2006). However, nitrification rates did peak at locations and times with intermediate WFPS, from 60 to 70%. The percent of net N mineralization that was due to nitrification decreased above 60% WFPS. Thus, diminished oxygen availability likely did limit the nitrification of mineralized ammonium, but not the total amount of dissolved inorganic N mineralized from organic N. Hefting and others (2004) documented a similar pattern of mostly ammonification with shallow groundwater and mostly nitrification with deeper groundwater in riparian soils. Some additional support for oxygen limitation of N transformations was suggested by the finding of greater ammonification and less percent nitrification in soils with finer texture. Finer textured soils have reduced oxygen availability than coarser soils (Groffman and Tiedje 1991). Floodplain locations with greater clay content likely had lower soil redox, stimulating preservation of mineralized NH_4^+ and limiting nitrification. In summary, microbial degradation of organic matter continued in fine textured and wet floodplain soils even when oxygen availability was insufficient to nitrify mineralized ammonium.

Net P mineralization in acidic wetland soils is the result of both microbial degradation of organic P and microbial reduction of metal complexes that desorb orthophosphate. In the floodplains of Difficult Run, the correlations of P mineralization with soil pH, ammonification, and texture suggest desorption under reducing conditions as the dominant pathway for orthophosphate production. We found that P mineralization rates increased as soil pH decreased. Lower pH increases the release of orthophosphate from iron minerals in reducing soils (Patrick and others 1973) and has been shown to increase P mineralization in wetlands (Verhoeven and others 1990). In addition, the strong positive association of P mineralization with net ammonification and negative association with coarse textured soils also suggest that the lack of oxygen in reducing soils resulted in greater desorption of SRP. However, some support for the role of microbial degradation of organic P as a source of mineralized P was found in the correlation of P turnover with soil organic content and nutrient stoichiometry. Faster turnover of soil P pools was found in soils that were generally more organic, specifically with greater C:P and N:P, suggesting that soil microbes may be relying on mineralizing organic P to supply their inorganic P needs. In fact, the greater turnover of P in more

organic soils suggests that organic P is more labile than mineral P—measured as net flux using the in situ modified resin core mineralization technique in the short hydroperiod floodplains of Difficult Run.

Pool Size and Quality of Organics

The amount and quality of organic material influenced floodplain soil net N mineralization rates. As soil organic matter and associated soil nutrient content increased (and bulk density decreased) along floodplain spatial gradients, the production of soil NH_4^+ and $\text{NH}_4^+ + \text{NO}_3^-$ increased. Soil organic and nutrient content is frequently identified as a control of N mineralization (Verhoeven and others 1990, 2001; Van Cleve and others 1993; Updegraff and others 1995; Bridgham and others 1998).

However, N turnover rates were similar across the lateral and longitudinal dimensions of the floodplains. Annual N turnover is calculated as the amount of inorganic N produced relative to the pool of soil TN. In other words, greater N mineralization rates were found in locations with larger pools of soil organic N. The relatively constant rate of N turnover suggests that the microbial capacity to mineralize organic N does not respond to the hydrogeomorphic gradients in these floodplains—more N is mineralized where more N is available, and not that microbes mineralize more of the available soil N. The floodplain of Difficult Run is relatively homogenous in soil and vegetation characteristics along lateral and longitudinal gradients. Conversely, large contrasts in soil characteristics among regional wetland types lead to large differences in N turnover rates (Bridgham and others 1998).

We did find that soil N turnover increased in locations with greater standing stocks of C, N, and P in peak herbaceous plant biomass, an index of herbaceous litter production and nutrient inputs to the soil. Herbaceous litter production is a small component of total litter production in the forested floodplains of Difficult Run, although largely composed of non-native species that are potentially increasing as in many urban forested ecosystems (Rybicki and others, unpublished data). The faster decomposition of soil N in locations with greater herbaceous production suggests that herbaceous litter is more labile than litter produced by the deciduous overstory trees. The molar C:N ratio of herbaceous litter (mean 22) was far less than that of overstory litterfall (mean 44; Rybicki and others, unpublished data). However, soil C:N and herbaceous C:N ratios were unrelated. Thus, inputs of

higher quality herbaceous litter stimulated the rate that soil N was mineralized (for example, Scott and Binkley 1997). Alternatively, greater availability of N stimulated production of herbaceous plants. Greater production of plant litter in floodplains is often associated with greater soil N mineralization rates (Burke and others 1999; Olde Venterink and others 2002; Wassen and others 2002; Follstad Shah and Dahm 2008) in what may be a positive feedback cycle.

Earthworms

Greater abundance of non-native earthworms has been found to increase potential net N mineralization rates in upland soils (Steinberg and others 1997; Szlavecz and others 2006) and increase nitrification in riparian soils (Costello and Lamberti 2009) of North America. In the Difficult Run floodplains, average worm density (126 individuals m^{-2} , unpublished data) and worm mass were similar to other riparian soils (Costello and Lamberti 2009), whereas worm density was similar but worm mass was much less than suburban upland soils in the mid-Atlantic USA (Szlavecz and others 2006). The earthworms in this study were dominated by non-native species (M. Lowit, USGS, unpublished data). The lack of a relationship between soil earthworm abundance and in situ N or P mineralization in this study may be due to the relatively wet floodplain soils, which may decrease earthworm abundance relative to upland soils and resulted in stronger control over microbial activity by soil organic content and moisture content that superseded any earthworm effects.

Wetland Nutrient Mineralization Rates

Because floodplains can trap large proportions of annual river loads (Noe and Hupp 2009), making accurate measurements of nutrient mineralization is critical to the development of floodplain N and P budgets (Andersen and others 2003; Wassen and Olde 2006; Kronvang and others 2009). The long-term fate of nutrient deposition in floodplains in part depends on hydrogeomorphic-driven variation in mineralization rates because dissolved nutrients are more mobile than particulate nutrients. For example, mineralization can produce large pools of soil nitrate that may be leached from floodplain soils into groundwater flowpaths and to the river (Bechtold and others 2003).

Floodplain soil in situ mineralization rates in Difficult Run are similar or lower than typical values for N and P, respectively, in other wetlands. A compilation of published field mineralization

measurements in wetland soils (digital Appendix 1 of Supplementary material) found that median minimum and maximum net N mineralization rates were 469 and 2326 $\mu\text{mol N m}^{-2} \text{d}^{-1}$, and for net P mineralization were 4 and 107 $\mu\text{mol P m}^{-2} \text{d}^{-1}$. In this study, net N mineralization averaged 873 and ranged from 244 to 2311 $\mu\text{mol N m}^{-2} \text{d}^{-1}$, and net P mineralization averaged 10 and ranged from 3 to 33 $\mu\text{mol P m}^{-2} \text{d}^{-1}$. The relatively low net P mineralization rates found in the urban Piedmont floodplains of Difficult Run may be due to their high mineral content and short hydroperiod compared to most wetland soils and likely abundance of orthophosphate-sorbing iron and aluminum oxides which prevent the accumulation of mineralized P in extractable soil solution.

Nutrient Turnover

Measured mineralization rates indicate that existing pools of floodplain soil N and P have long turnover times, averaging 22 years (0.046 y^{-1} ; range 8–58 years) for N and 369 years for P (0.0027 y^{-1} ; range 104–1558 years). These turnover times are similar to those found at the mid-watershed site in Difficult Run prior to this study (Noe 2011), indicating repeatability among years. Turnover of soil N was relatively slow in the Difficult Run floodplain compared to other wetlands, which typically ranged from 10 to 26 years (digital Appendix 1 of Supplementary material). We found no published rates of in situ soil P turnover in wetlands. The stability of soil N, and in particular P, suggests that most inputs of nutrients through sedimentation, as well as existing pools of soil nutrients, are likely retained for a long time in the floodplain of Difficult Run and other floodplains with mineral soil. Vegetative litter N and P production fluxes were similar to or exceeded soil nutrient mineralization rates (Rybicki and others, unpublished data), suggesting efficient recycling of N and P within the floodplain ecosystem (Hefting and others 2005). However, herbaceous vegetation was associated with greater conversion of soil N pools into dissolved inorganic N fractions, which could be exported from floodplain soils into the river channel and transported downstream. Therefore, targeting tree planting as a riparian restoration method would enhance sequestration of soil N by reducing turnover rates compared to an herbaceous vegetation community. Although the slow turnover of floodplain soil nutrients is likely good for downstream water quality in the short term, the large reservoir of floodplain nutrients could be exported downstream over the long term

to sensitive aquatic ecosystems such as the Chesapeake Bay.

CONCLUSIONS

There was a direct functional linkage between hydrologic connectivity and biogeochemical process rates through the filter of floodplain geomorphic units. Lateral and longitudinal gradients in river hydrologic connectivity influenced floodplain soil N and P mineralization rates by changing inputs of water, nutrients, sediment, and vegetative litterfall, as well as soil characteristics. Although lateral gradients in mineralization and ecosystem characteristics among geomorphic units were more pronounced, longitudinal gradients from the headwaters to the mouth of the watershed were also evident. Greater inputs of sediment and inorganic nutrients associated with flooding increased both N and P mineralization in floodplain soils, indicating that hydrologic connectivity can subsidize floodplain fertility. These findings indicate that the geomorphic functional units in floodplain systems (Amoros and others 1987; Ward 1989; Stanford and others 2005) can have inherently different biogeochemical process rates due to differences in the inputs, quantity, and quality of soil organic matter and nutrients. Our findings contribute to the body of knowledge on how hydrologic connectivity influences floodplain biogeochemical fluxes and community structure, including nutrient sedimentation (Craft and Casey 2000; Noe and Hupp 2005), denitrification (Richardson and others 2004; Forshay and Stanley 2005; Welti and others 2012), NO_3^- uptake by biota (Heiler and others 1995), soil P sorption (Bridgman and others 2001), aquatic invertebrates (Arscott and others 2005; Reese and Batzer 2007), and vegetation (Lite and others 2005; Renöfält and others 2005).

ACKNOWLEDGMENTS

This research was supported by the USGS Chesapeake Priority Ecosystem Science, Hydrologic Networks & Analysis, and National Research Programs. We thank Nicholas Ostroski, Kristin Wolf, Ed Schenk, Myles Robinson, Mike Lowit, Krystal Belaling J. V. Loperfido, Dianna Hogan, and Meghan Fellows for their valuable contributions to its completion, and J. V. Loperfido and Camille Staggs for their constructive reviews of the manuscript. Any use of trade, product, or firm names is for descriptive purposes only and does not imply endorsement by the US Government.

REFERENCES

- Adair EC, Binkley D, Andersen D. 2004. Patterns of nitrogen accumulation and cycling in riparian floodplain ecosystems along the Green and Yampa rivers. *Oecologia* 139:108–16.
- Amoros C, Bornette G. 2002. Connectivity and biocomplexity in waterbodies of riverine floodplains. *Freshw Biol* 47:761–76.
- Amoros C, Roux AL, Reygrobellet JL, Bravard JP, Pautou G. 1987. A method for applied ecological studies of fluvial hydrosystems. *Regul Rivers* 1:17–36.
- Andersen DC, Nelson SM, Binkley D. 2003. Flood flows, leaf breakdown, and plant-available nitrogen on a dryland river floodplain. *Wetlands* 23:180–9.
- Arscott DB, Tockner K, Ward JV. 2005. Lateral organization of aquatic invertebrates along the corridor of a braided floodplain river. *J North Am Benthol Soc* 24:934–54.
- Axt JR, Walbridge MR. 1999. Phosphate removal capacity of palustrine forested wetlands and adjacent uplands in Virginia. *Soil Sci Soc Am J* 63:1019–31.
- Bechtold JS, Edwards RT, Naiman RJ. 2003. Biotic versus hydrologic control over seasonal nitrate leaching in a floodplain forest. *Biogeochemistry* 63:53–72.
- Bechtold SJ, Naiman RJ. 2006. Soil texture and nitrogen mineralization potential across a riparian toposequence in a semi-arid savanna. *Soil Biol Biochem* 38:1325–33.
- Binkley D, Hart SC. 1989. The components of nitrogen availability assessments in forest soils. *Adv Soil Sci* 10:57–112.
- Bridgman SD, Updegraff K, Pastor J. 1998. Carbon, nitrogen, and phosphorus mineralization in northern wetlands. *Ecology* 79:1545–61.
- Bridgman SD, Johnston CA, Schubauer-Berigan JP, Weishampel P. 2001. Phosphorus sorption dynamics in soils and coupling with surface and pore water in riverine wetlands. *Soil Sci Soc Am J* 65:577–88.
- Brinson MM. 1993. Changes in the functioning of wetlands along environmental gradients. *Wetlands* 13:65–74.
- Brunland GL, Richardson CJ. 2004. A spatially explicit investigation of phosphorus sorption and related soil properties in two riparian wetlands. *J Environ Qual* 33:785–94.
- Burke MK, Lockaby BG, Conner WH. 1999. Aboveground production and nutrient circulation along a flooding gradient in a South Carolina Coastal Plain forest. *Can J For Res* 29:402–1418.
- Clawson RG, Lockaby BG, Rummer B. 2001. Changes in production and nutrient cycling across a wetness gradient within a floodplain forest. *Ecosystems* 4:126–38.
- Costello DM, Lamberti GA. 2009. Biological and physical effects of non-native earthworms on nitrogen cycling in riparian soils. *Soil Biol Biochem* 41:2230–5.
- Craft CB, Casey WP. 2000. Sediment and nutrient accumulation in floodplain and depressional freshwater wetlands of Georgia, USA. *Wetlands* 20:323–32.
- Follstad Shah JJ, Dahm CN. 2008. Flood regime and leaf fall determine soil inorganic nitrogen dynamics in semiarid riparian forests. *Ecol Appl* 18:771–88.
- Forshay KJ, Stanley EH. 2005. Rapid nitrate loss and denitrification in a temperate river floodplain. *Biogeochemistry* 75:43–64.
- Groffman PM, Tiedje JM. 1991. Relationships between denitrification, CO_2 production and air-filled porosity in soils of different texture and drainage. *Soil Biol Biochem* 23:299–302.

- Hefting M, Clément JC, Dowrick D, Cosandey AC, Bernal S, Cimpian C, Tatur A, Burt TP, Pinay G. 2004. Water table elevation controls on soil nitrogen cycling in riparian wetlands along a European climatic gradient. *Biogeochemistry* 67:113–34.
- Hefting M, Clement JC, Bienkowski P, Dowrick D, Guenat C, Butturini A, Topa S, Pinay G, Verhoeven JTA. 2005. The role of vegetation and litter in the nitrogen dynamics of riparian buffer zones in Europe. *Ecol Eng* 24:465–82.
- Heiler G, Hein T, Schiemer F, Bornette G. 1995. Hydrological connectivity and flood pulses as the central aspects for the integrity of a river–floodplain system. *Regul Rivers Res Manag* 11:351–61.
- Hopkinson CS. 1992. A comparison of ecosystem dynamics in freshwater wetlands. *Estuaries Coasts* 15:549–62.
- Hupp CR. 2000. Hydrology, geomorphology and vegetation of Coastal Plain rivers in the south-eastern USA. *Hydrol Process* 14:2991–3010.
- Hupp CR, Demas CR, Kroes DE, Day RH, Doyle TW. 2008. Recent sedimentation patterns within the central Atchafalaya Basin, Louisiana. *Wetlands* 28:125–40.
- Johnston CA, Bridgman SD, Schubauer-Berigan JP. 2001. Nutrient dynamics in relation to geomorphology of riverine wetlands. *Soil Sci Soc Am J* 65:557–77.
- Jolley RL, Lockaby BG, Governo RM. 2010. Biogeochemical influences associated with sedimentation in riparian forests of the Southeastern Coastal Plain. *Soil Sci Soc Am J* 74:326–36.
- Junk WJ, Bayley PB, Sparks RE. 1989. The flood pulse concept in river–floodplain systems. *Can Sp Pub Fish Aquat Sci* 106:110–27.
- Kroes D, Hupp C, Noe G. 2007. Sediment, nutrient, and vegetation trends along the tidal, forested Pocomoke River, Maryland. In: Conner WH, Doyle TW, Krauss KW, Eds. *Ecology of tidal freshwater forested wetlands of the South-eastern United States*. New York: Springer. p 113–37.
- Kronvang B, Hoffmann CC, Drøge R. 2009. Sediment deposition and net phosphorus retention in a hydraulically restored lowland river floodplain in Denmark: combining field and laboratory experiments. *Mar Freshw Res* 60:638–46.
- Lewis WMJ, Hamilton SK, Lasi MA, Rodriguez M, Saunders JFI. 2000. Ecological determinism on the Orinoco floodplain. *Bioscience* 50:681–92.
- Lite SJ, Bagstad KJ, Stromberg JC. 2005. Riparian plant species richness along lateral and longitudinal gradients of water stress and flood disturbance, San Pedro River, Arizona, USA. *J Arid Environ* 63:785–813.
- Lockaby BG, Governo R, Schilling E, Cavalcanti G, Hartsfield C. 2005. Effects of sedimentation on soil nutrient dynamics in riparian forests. *J Environ Qual* 34:390–6.
- Lyons JB, Gorres JH, Amador JA. 1998. Spatial and temporal variability of phosphorus retention in a riparian forest soil. *J Environ Qual* 27:895–903.
- McIntyre RES, Adams MA, Grierson PF. 2009. Nitrogen mineralization potential in rewetted soils from a semi-arid stream landscape, north-west Australia. *J Arid Environ* 73:48–54.
- Mouw JEB, Stanford JA, Alaback PB. 2009. Influences of flooding and hyporheic exchange on floodplain plant richness and productivity. *River Res Appl* 25:929–45.
- Mulvaney RL. 1996. Nitrogen-inorganic forms. In: Sparks DL, Ed. *Methods of soil analysis, part 3, chemical methods*. Madison: SSSA and ASA. p 1085–122.
- Noe GB. 2011. Measurement of net nitrogen and phosphorus mineralization in wetland soils using a modification of the resin-core technique. *Soil Sci Soc Am J* 75:760–70.
- Noe GB. 2013. Interactions among hydrogeomorphology, vegetation, and nutrient biogeochemistry in floodplain ecosystems. In: Shroder J, Jr., Hupp C, Butler D, Eds. *Treatise on geomorphology*. San Diego: Academic Press.
- Noe GB, Hupp CR. 2005. Carbon, nitrogen, and phosphorus accumulation in floodplains of Atlantic Coastal Plain rivers, USA. *Ecol Appl* 15:1178–90.
- Noe GB, Hupp CR. 2009. Retention of riverine sediment and nutrient loads by Coastal Plain floodplains. *Ecosystems* 12:728–46.
- Olde Venterink H, Pieterse NM, Belgers JDM, Wassen MJ, de Ruiter PC. 2002. N, P, and K budgets along nutrient availability and productivity gradients in wetlands. *Ecol Appl* 12:1010–26.
- Olde Venterink H, Vermaat JE, Pronk M, Wiegman F, van der Lee GEM, van den Hoorn MW, Higler LWG, Verhoeven JTA. 2006. Importance of sediment deposition and denitrification for nutrient retention in floodplain wetlands. *Appl Veg Sci* 9:163–74.
- Patrick JWH, Gotoh S, Williams BG. 1973. Strengite dissolution in flooded soils and sediments. *Science* 179:564–5.
- Petts GE, Gurnell AM, Gerrard AJ, Hannah DM, Hansford B, Morrissey I, Edwards PJ, Kollmann J, Ward JV, Tockner K. 2000. Longitudinal variations in exposed riverine sediments: a context for the ecology of the Fiume Tagliamento, Italy. *Aquat Conserv Mar Freshw Ecosyst* 10:249–66.
- Pinay G, Fabre A, Vervier P, Gazelle F. 1992. Control of C, N, P distribution in soils of riparian forests. *Landscape Ecol* 6:121–32.
- Pinay G, Black VJ, Planty-Tabacchi AM, Gumiero B, Decamps H. 2000. Geomorphic control of denitrification in large river floodplain soils. *Biogeochemistry* 50:163–82.
- Pizzuto JE. 1987. Sediment diffusion during overbank flows. *Sedimentology* 34:301–17.
- Poole GC. 2010. Stream hydrogeomorphology as a physical science basis for advances in stream ecology. *J North Am Benthol Soc* 29:12–25.
- Reddy KR, Wang Y, DeBusk WF, Fisher MM, Newman S. 1998. Forms of soil phosphorus in selected hydrologic units of the Florida Everglades. *Soil Sci Soc Am J* 62:1134–47.
- Reese EG, Batzer DP. 2007. Do invertebrate communities in floodplains change predictably along a river's length? *Freshw Biol* 52:226–39.
- Renöfält BM, Nilsson C, Jansson R. 2005. Spatial and temporal patterns of species richness in a riparian landscape. *J Biogeogr* 32:2025–37.
- Richardson WB, Strauss EA, Bartsch LA, Monroe EM, Cavanaugh JC, Vingum L, Soballe DM. 2004. Denitrification in the Upper Mississippi River: rates, controls, and contribution to nitrate flux. *Can J Fish Aquat Sci* 61:1102–12.
- Robertson GP, Sollins P, Ellis BG, Lajtha K. 1999. Exchangeable ions, pH, and cation exchange capacity. In: Robertson GP, Coleman DC, Bledsoe CS, Sollins P, Eds. *Standard soil methods for long-term ecological research*. New York: Oxford University Press. p 106–14.
- Scott NA, Binkley D. 1997. Foliage litter quality and annual net N mineralization: comparison across North American forest sites. *Oecologia* 111:151–9.

- Sleutel S, Moeskops B, Huybrechts W, Vandebossche A, Salomez J, De Bolle S, Buchan D, De Neve S. 2008. Modeling soil moisture effects on net nitrogen mineralization in loamy wetland soils. *Wetlands* 28:724–34.
- Sparks RE, Nelson JC, Yin Y. 1998. Naturalization of the flood regime in regulated rivers. *Bioscience* 48:706–20.
- Spink A, Sparks RE, van Oorschot M, Verhoeven JTA. 1998. Nutrient dynamics of large river floodplains. *Regul Rivers Res Manag* 14:203–16.
- Stanford JA, Lorang MS, Hauer FR. 2005. The shifting habitat mosaic of river ecosystems. *Verh Int Ver Theor Angew Limnol* 29:123–36.
- Stanley EH, Fisher SG, Grimm NB. 1997. Ecosystem expansion and contraction in streams. *Bioscience* 47:427–35.
- Steiger J, Gurnell AM. 2002. Spatial hydrogeomorphological influences on sediment and nutrient deposition in riparian zones: observations from the Garonne River, France. *Geomorphology* 49:1–23.
- Steinberg DA, Pouyat RV, Parmelee RW, Groffman PM. 1997. Earthworm abundance and nitrogen mineralization rates along an urban–rural land use gradient. *Soil Biol Biochem* 29:427–30.
- Stoeckel DM, Miller-Goodman MS. 2001. Seasonal nutrient dynamics of forested floodplain soil influenced by microtopography and depth. *Soil Sci Soc Am J* 65:922–31.
- Surridge BWJ, Heathwaite AL, Baird AJ. 2007. The release of phosphorus to porewater and surface water from river riparian sediments. *J Environ Qual* 36:1534–44.
- Szlavec K, Placella SA, Pouyat RV, Groffman PM, Csuzdi C, Yesilonis I. 2006. Invasive earthworm species and nitrogen cycling in remnant forest patches. *Appl Soil Ecol* 32:54–62.
- Updegraff K, Pastor J, Bridgman SD, Johnston CA. 1995. Environmental and substrate controls over carbon and nitrogen mineralization in northern wetlands. *Ecol Appl* 5:151–63.
- US Geological Survey. 2007. Water-data report 2007, 01646000 Difficult Run near Great Falls. Reston: Geological Survey.
- Van Cleve K, Yarie J, Erickson R, Dyrness C. 1993. Nitrogen mineralization and nitrification in successional ecosystems on the Tanana River floodplain, Interior Alaska. *Can J For Res* 23:970–8.
- Verhoeven JTA, Maltby E, Schmitz MB. 1990. Nitrogen and phosphorus mineralization in fens and bogs. *J Ecol* 78:713–26.
- Verhoeven JTA, Whigham DF, van Logtestijn R, O'Neill J. 2001. A comparative study of nitrogen and phosphorus cycling in tidal and non-tidal riverine wetlands. *Wetlands* 21:210–22.
- Ward JV. 1989. Riverine-wetland interactions. In: Sharitz RR, Gibbons JW, Eds. *Freshwater wetlands and wildlife*. Oak Ridge: USDOE Office of Scientific and Technical Information. p 385–400.
- Wassen MJ, Olde Venterink H. 2006. Comparison of nitrogen and phosphorus fluxes in some European fens and floodplains. *Appl Veg Sci* 9:213–22.
- Wassen MJ, Peeters WHM, Olde Venterink H. 2002. Patterns in vegetation, hydrology, and nutrient availability in an undisturbed river floodplain in Poland. *Plant Ecol* 165:27–43.
- Welti N, Bondar-Kunze E, Singer G, Tritthart M, Zechmeister-Boltenstern S, Hein T, Pinay G. 2012. Large-scale controls on potential respiration and denitrification in riverine floodplains. *Ecol Eng* 42:73–84.
- Wharton CH, Kitchens WM, Pendleton EC, Sipe TW. 1982. *The ecology of bottomland hardwood swamps of the Southeast: a community profile*. Washington, DC: US Fish and Wildlife Service. 133 pp.
- Whigham DF, Chitterling C, Palmer B. 1988. Impacts of freshwater wetlands on water quality: a landscape perspective. *Environ Manage* 12:663–71.
- Wolf K, Ahn C, Noe GB. 2011a. Microtopography enhances nitrogen cycling and removal in created wetlands. *Ecol Eng* 37:1398–406.
- Wolf K, Ahn C, Noe GB. 2011b. Development of soil properties and nitrogen cycling in created wetlands. *Wetlands* 31:699–712.